

# **SENSITIVITY ANALYSES OF PUMPING TEST IN SALT-FRESH WATER AQUIFER 2: DRAWDOWN AND JOINT CONFIDENCE REGIONS**

L. LEBBE<sup>1</sup> & N. VAN MEIR<sup>2</sup>

1 Fund of Scientific Research-Flanders  
2 Dept. of Geology and Pedology- Ghent University  
Laboratory of Applied Geology and Hydrogeology, Ghent University  
Krijgslaan, 281 (S8) B-9000 Belgium

## **ABSTRACT**

Using an inverse numerical model HYPARIDEN it is examined if the planned observation wells provide sufficient data to infer the vertical and horizontal conductivities along with the specific elastic storage. Utilising an axial-symmetric numerical model the drawdowns which would occur in the planned observation well are generated and an error is added. With the inverse numerical model the optimal values of the three hydraulic parameters are deduced along with a number of statistical parameters. The relations between these statistical parameters and the approximate joint confidence region are given. It is shown that the planned observation wells will generate a well-posed problem for the identification of the hydraulic parameters. From the drawdown data the horizontal conductivity can be inferred with the highest accuracy, the vertical conductivity with the smallest accuracy. By the adding the concentration sensitivities, as calculated with the MOCDENS3D model, the hydraulic parameter identification problem becomes even better posed. The concentration data describing the rise of the fresh-salt water transition zone provide valuable data for the inference of the vertical conductivities and so enrich the parameter identification problem.

## **INTRODUCTION**

The present paper is the second part of a preliminary study for the development of an inverse model interpreting a pumping test in a multi-layered aquifer filled with salt and fresh water. With this model the optimal parameter values are determined using the observed evolution of the fresh water heads. Besides the optimal values a joint confidence region of the parameters can be inferred.

In the first part of this preliminary study the sensitivities of the concentrations observed in the vicinity of the salt-fresh transition zone with respect to the hydraulic parameters and the transport parameters is studied. In this second part the sensitivities of the drawdowns to the hydraulic parameters are inspected. The drawdowns are considered in six observation wells.

Three observation wells are situated in the directly pumped part of the groundwater reservoir at different distances from the pumped well and three are situated above and below this part. The drawdowns are calculated with an axial-symmetric model in which the subdivision of the ground water reservoir in layers is the same as in the MOCDENS3D model. On the logarithm of the generated drawdown an error is added with a mean equal to zero and a standard deviation of 0.01. These data are inserted in the inverse numerical model. The iterations of the inverse numerical model are then followed. The optimal values of three hydraulic parameters can be inferred: the horizontal and vertical conductivities and the specific elastic storages along with some statistical parameters characterising the joint confidence region. To study the complementarity of

the information provided by the drawdowns and the concentration changes the condition indexes and the matrix of marginal variance proportion deduced from three different sensitivity matrixes are compared. In the first case only the drawdown sensitivities are considered; in the second case the drawdown sensitivities are combined with the concentration sensitivities and in the third case only the concentration sensitivities are considered

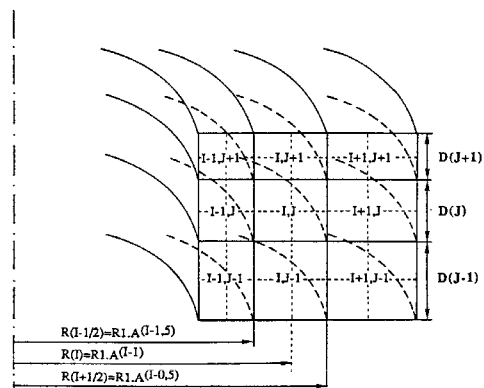
## PRINCIPLES OF HYDPARIDEN

HYDPARIDEN (Lebbe, 1999) is an inverse numerical model that infers the optimal values of hydraulic parameters and their joint confidence area based on drawdowns measured during a pumping test in a multi-layered aquifer. In this inverse model it is now also possible to include residuals and sensitivities that were calculated with another model, e.g., obtained by MOCDENS3D (Oude Essink, 1998) as will be demonstrated in this paper. The inverse model is obtained by the combination of a numerical model with sensitivity analyses and a non-linear regression.

### Numerical model

The applied numerical model is an axial-symmetric model in which the groundwater reservoir can be subdivided in a large number of layers. Each layers has a arge lateral extension and is supposed to be homogeneous. The rings are subdivided in a number of coaxial rings. Each layer is characterised by a horizontal and vertical conductivity and a specific elastic storage. The bottom layer is bounded by an impermeable boundary and the top layer by a water table. The inner boundary is either a constant flux boundary or an impermeable boundary. The constant flux boundaries correspond with directly pumped layers, the impermeable boundaries indirectly pumped layer without

well screen. The drawdown increase in the outermost ring of each layer is derived by extrapolation of the drawdown increase of three rings before the outermost during the former time step. The drawdowns are calculated in nodal circles and at different time steps. The nodal circles are situated at half height of the rings and their radii are equal to the geometric mean of the inner and outer radii of the rings (fig. 1). The inner and outer radii of the rings form a logarithmic increasing series. The increase with a factor A (mostly  $10^{0.1}$ ). During the calculations a continuous linear change is assumed between the drawdowns of two successive nodal circles of the same layer and the logarithm of the distance to the pumped well. The first considered time steps are very small. The length of the consecutive time steps increase also with the factor A. During the calculation a linear course is assumed between the drawdown and the logarithm of the time since starting the pump.



**Figur 1 Ring I,J and surrounding rings of the axial-symmetric grid. R1 is the initial radius and A is a factor >1**

In Lebbe (1999) the numerical model is validated by the model of Theis (1935), Jacob (1946), Hantush (1960,1966) and the model of Boulton (1963) as explained by Cooley (1971,1972) and Cooley and Case (1973). In Lebbe and De Breuck (1995) the validation is treated with one special case of the Hantush (1960) model.

## Residuals and Sensitivities

The residuals are defined as:

$$r = \log_{10} s^* - \log_{10} \hat{s} \quad (1)$$

where  $\mathbf{r}$  are the residuals,  $\mathbf{s}^*$  the measured drawdowns, and  $\hat{\mathbf{s}}$  the calculated drawdowns.

The sensitivities  $J_{ij}$  of the drawdown  $s_i$  to the hydraulic parameters or group of parameters,  $hp_j$ , are defined as follows:

$$J_{ij} = \frac{\log_{10} \hat{s}_i(hp_j \cdot sf) - \log_{10} \hat{s}_i}{\log_{10} sf} \quad (2)$$

where  $sf$  is the sensitivity factor;  $\hat{s}_i$  is the calculated drawdown corresponding with the  $i^{\text{th}}$  observation using the initial parameter estimates or obtained with the foregoing iteration; and  $\hat{s}_i(hp_j \cdot sf)$  is the calculated drawdown corresponding with the  $i^{\text{th}}$  observation using the parameter estimates except for the estimate(s) of the  $j^{\text{th}}$  parameter of which the estimate(s) is (are) multiplied by the sensitivity factor. The hydraulic parameters are viewed in their logarithmic space due to their large variation.

## Adjustment of parameter values

With the linearisation method (Draper and Smith, 1981) the adjustment factors are derived from the residuals and the sensitivities.

$$\mathbf{A} = (\mathbf{J}^T \mathbf{J})^{-1} \mathbf{J}^T \mathbf{r} \quad (3)$$

where  $\mathbf{A}$  is the vector of the logarithms of the parameter adjustment factors. The new estimates of the parameter values are obtained by multiplying the old ones by their corresponding adjustment factors, or:

$$hp_j^{m+1} = hp_j^m \cdot 10^{A_j^m} \quad (4)$$

where  $hp_j^m$  is the value of the  $j^{\text{th}}$  parameter and the  $m^{\text{th}}$  iteration of the inverse process,  $A_j^m$  is the logarithm of the adjustment factor of the  $j^{\text{th}}$  parameter and of the  $m^{\text{th}}$  iteration. The algorithm is repeated until the adjustment factors become very small and the sum of the squared residuals (the object function) reaches a minimum value.

## Statistical parameters

When it is assumed that the residuals approximate a normal distribution with a mean equal to zero, and that the drawdowns can be approximated as a linear function within the considered region, then the joint probability distribution can be described by the optimal values and the covariance matrix of the parameters  $\text{cov}_p$ :

$$\text{cov}_p = \sigma_s^2 (\mathbf{J}^T \mathbf{J})^{-1} \quad (5)$$

where  $\sigma_s^2$  can be estimated as  $(\sum_{i=1}^n r_i^2)/(n-p)$  when  $n$  is the number of observations and  $p$  the number of parameters. The marginal standard deviation  $sm_j$  of the  $j^{\text{th}}$  parameter is the square root of the  $j^{\text{th}}$  diagonal term of the covariance matrix (Carrera and Neuman, 1986). The partial correlation coefficient between the parameters  $hp_j$  and  $hp_{j+1}$  is  $\text{cov}_{p,j,j+1}/(sm_j \cdot sm_{j+1})$ .

The conditional standard deviations  $\mathbf{sc}$  can be approximated using the eigenvalues and the eigenvectors of the covariance matrix (Lebbe, 1988):

where  $\alpha_k$  is the  $k^{\text{th}}$  eigenvalue of the

$$S_{CJ} = (\sum_{k=1}^p \beta_{jk}^2 / \alpha_k)^{-1/2} \quad (6)$$

covariance matrix and  $\beta_{jk}$  is the  $jk^{\text{th}}$  eigenvector of the covariance matrix. The conditional standard deviations help to locate the intersections of the parameter axes, which go through the optimal values and the bounds of the approximate joint confidence region, which is drawn following the linearisation method (e.g., fig. 3)

Besides the marginal and conditional standard deviation and the partial correlation coefficients, the condition indices and the matrix of marginal variance-decomposition proportions are also collinear diagnostic tools. According to Belsley (1990), the marginal variance of the  $j^{\text{th}}$  hydraulic parameter  $\text{var}_{m_j}$  can be written as:

where  $\mu_j$  is the  $j^{\text{th}}$  singular value of the

$$\text{var}_{m_j} = \sigma_s^2 \sum_{k=1}^p v_{jk}^2 / \mu_j^2 \quad (7)$$

sensitivity matrix  $\mathbf{J}$  and  $\mathbf{u}_{jk}$  is the  $jk^{\text{th}}$  eigenvector of the Hessian matrix  $\mathbf{J}^T \mathbf{J}$ .

The proportion of the marginal variance of the hydraulic parameter  $hp_j$  associated with the  $k^{\text{th}}$  singular value is given by:

$$\pi_{jk} = \frac{\phi_{jk}}{\phi_j} \text{ with } \phi_{jk} = \frac{v_{jk}^2}{\mu_k^2} \quad (8)$$

$$\text{and } \phi_j = \sum_{k=1}^p \phi_{jk}$$

The proportion is associated with a condition index  $\eta_k$ , which is the ratio of the largest singular value ( $\mu_{\text{max}}$ ) to the singular value  $\mu_k$  ( $\eta_k = \mu_{\text{max}}/\mu_k$ ). The largest value of  $\eta_k$  is called the condition number of  $\mathbf{J}$ .

Belsley (1990) extends the Kendall-Silvey suggestion as follows: there are as many near dependencies among the columns of the sensitivity matrix  $\mathbf{J}$  as there are high condition indices. Weak dependencies are associated with condition indices around 5-10, whereas moderate to strong relations are associated with condition indices of 30-100. Small singular values of the matrix  $\mathbf{J}$  and consequently large condition indices correspond with large eigenvalues of the matrix  $(\mathbf{J}^T \mathbf{J})^{-1}$  and with large principal axes of the approximate joint confidence region.

Once the near dependencies are found, the columns of the sensitivity matrix  $\mathbf{J}$  or the hydraulic parameters must be identified which are involved in these dependencies. If only one condition index is very large with respect to the others, the hydraulic parameters that are involved in the dependencies are those showing large marginal variance decomposition proportions. In the case of different large condition indices, the columns involved in one or the other group of near dependency are determined by addition of the proportions corresponding with these large condition indices. The identification of the columns that form the same group of near dependency cannot be distinguished from the proportions alone (Tarhouni, 1994). Therefore, Belsley (1990) proposed to use the partial correlation coefficient between the involved columns along with the

proportions to identify the columns that form a group of near dependency.

### Joint confidence area

For nonlinear problems the exact joint confidence region is obtained by drawing the contour lines of the sums of the squared residuals calculated for different parameter combinations. The values of these contour lines for different significance levels are inferred with following equation:

$$S(\hat{hp}) = S(\hat{hp}) \left(1 + \frac{p}{n-p} F(p, n-p, 1-\alpha)\right) \quad (9)$$

where  $S(\hat{hp})$  is the sum of the squared residuals corresponding to the optimal values of the hydraulic parameters,  $\hat{hp}$ , where  $p$  is the number of identified parameters,  $n$  is the number of observations and  $F(p, n-p, 1-\alpha)$  is the F-distribution for  $p$  and  $n-p$  degrees of freedom and a significance level  $1-\alpha$ . For each considered parameter combination the residuals are obtained after a complete simulation with the numerical model. These contours are exact confidence contours in the linear as well as in the nonlinear case. In the nonlinear case, the level of probability is approximated (Draper and Smith, 1981). Cross sections through the approximate joint confidence region are obtained when the residuals are first calculated using the residuals at the optimal solution and their sensitivities by the application of the linearisation method using following equation (Hill, 1989):

$$r(\hat{hp}) = r(\hat{hp}) + \hat{\mathbf{J}}(\hat{hp} - \hat{hp}) \quad (10)$$

where  $\hat{\mathbf{J}}$  is the sensitivity matrix corresponding with the optimal logarithmic values  $\hat{hp}$ . The obtained residuals are squared and summed for each parameter value set. The contour lines of these sums of the squared residuals represent the bounds of the approximate joint confidence region (see e.g., fig. 3). These bounds approximate the bounds of the exact joint confidence region when the residuals approximate a normal distribution with a zero mean and when the

drawdowns can be approximated as a linear function within the considered region. This is generally the case in pumping tests if this region is not too large. The approximate joint confidence regions are p-dimensional ellipsoids (p stands for number of identified parameters). The eigenvalues and eigenvectors of the covariance matrix, the marginal and conditional standard deviations, and the condition indexes all help in characterising the approximate joint confidence regions as will be demonstrated in this paper.

### **SYNTHETIC PROBLEM**

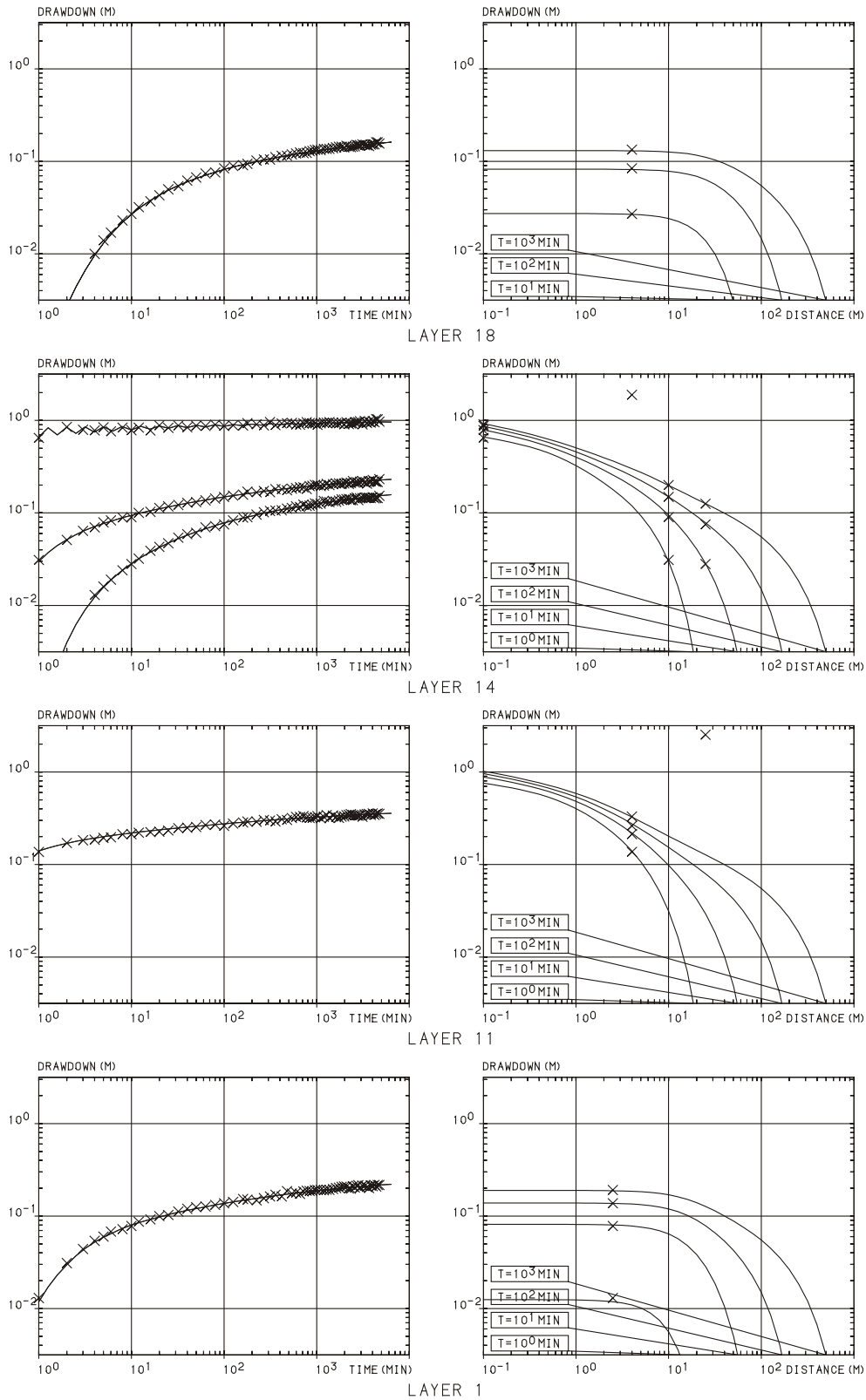
The same synthetic problem is treated as in part 1 of this study. There, the lithostratigraphic cross-section and the subdivision of the groundwater reservoir in layers of the numerical model is described. The same subdivision is used in the numerical model. The numbering of the layers is, however, different from the MOCDENS3D model. Here, the layers are numbered in the upward direction. Layer 1 corresponds with Layer 20 of the MOCDENS3D-model; Layer 2 with Layer 19 of MOCDENS3D; etc.

For the calculation of the 'synthetic' drawdowns the same horizontal and vertical conductivities are applied as in part 1 as well as the specific elastic storages and discharge rates for the different layers ( $Q_T = 95 \text{ m}^3/\text{d}$ ). The drawdowns are generated for six observation wells. Three observation wells are located in three different layers. Three wells are located in the directly pumped part of the groundwater reservoir at a distance of respectively 0.1, 10 and 25 m from the pumped well. One observation well is located in the bottom layer (Layer 1) at 2.5 m from the pumped well; one in Layer 11 and one in Layer 18 both at a distance of 4 m from the pumped well. The times at which the 'synthetic drawdowns' are calculated correspond with the times at which they were normally measured during a pumping test lasting three

days. The drawdowns are first calculated with the normal model. On the logarithm of these drawdowns errors were added. These errors have a normal distribution with a mean equal to zero and a standard deviation of 0.01. This means that 68% of the relative errors are situated between +2.33% and -2.33%. By the truncation of the drawdown to the millimetre some addition errors are added especially on the smaller drawdowns. On the 378 generated drawdowns thirteen drawdowns are smaller than 20 mm. The 'synthetic' drawdowns are represented by crosses in time-drawdown and in distance-drawdown graphs (fig. 2).

The inverse numerical model is first validated with these synthetic drawdown data. Three parameter groups are considered. The first parameter group includes the horizontal conductivities of all layers; the second groups all the vertical conductivities of all layers; and the third considers the specific elastic storages of all layers. The initial values of the hydraulic parameters are changed with respect to the values utilised for the calculation of the 'synthetic' drawdown. All horizontal and vertical conductivities are divided by two whereas the specific elastic storages of the layers are multiplied by three. According to these initial values the residuals, the object function (or sum of squared residuals) and the sensitivities are calculated by the perturbation method (Eq. 2).

Based on these residuals and the sensitivities the adjustment factors are calculated (Eq.3). All hydraulic parameters of a same group are multiplied by the same adjustment factor. The successive values of the hydraulic parameters during the iterations of the inverse model are given in Table 1 along with the decrease of the object function. The observed and calculated drawdowns corresponding with the optimal values are represented in fig. 2.



**Figur 2 Observed drawdown (crosses) and calculated drawdown (solid lines) corresponding with the optimal parameter values**

Table 1 Evolution of the object function and the parameter values during the iteration of the inverse numerical model

Iter. No	Hydraulic parameters			$\sum_1^{378} r_i^2$
	$K_h(1)$ m/d	$k_v(1)$ m/d	$s_s(1)$ m <sup>-1</sup>	
-	4.000	2.000	$3.00 \times 10^{-3}$	40.85
1	7.065	5.682	$2.39 \times 10^{-3}$	5.372
2	7.817	4.329	$1.15 \times 10^{-3}$	.1470
3	7.991	3.861	$1.01 \times 10^{-3}$	.0666
4	7.978	3.891	$1.03 \times 10^{-3}$	.0657
5	7.980	3.891	$1.03 \times 10^{-3}$	.0656
*	8.000	4.000	$1.00 \times 10^{-3}$	-

- initial values of hydraulic parameters

\* parameter values used to generate drawdown

After the optimisation of the problem it is found that the residuals exhibit a normal distribution with a mean equal to zero and standard deviation of 0.0132. Because the joint confidence region of hydraulic parameters is small (see further fig. 3 and 4) one can assume that the function is linear within this area and that the joint probability distribution can be described by the optimal values and the covariance matrix. From the covariance matrix, the partial correlation coefficients can be inferred (Table 2).

Table 2 Partial correlation coefficients along with conditional and marginal standard deviation  $s_c$  and  $s_m$ .

Para m.	$k_h(1)$	$k_v(1)$	$s_s(1)$	$s_c$	$s_m$
$k_h(1)$	1.000	-.0109	-.0792	0.0010	0.0011
$k_v(1)$	-.0109	1.000	-.4111	0.0021	0.0023
$s_s(1)$	-.0792	-.4111	1.000	0.0019	0.0021

The correlation coefficients are rather small. The conditional and the marginal standard deviations reveal that the horizontal conductivity can be inferred with the highest accuracy from the drawdown observations and the vertical conductivity with the smallest accuracy. The 99% approximate joint confidence region is a three-dimensional ellipsoid within the parameter space (Fig. 3). Three parameter axes are considered: the horizontal conductivities  $k_h$ , the vertical conductivities  $k_v$  and the specific elastic storage  $s_s$ . On the axes the parameter values are represented with

respect to their optimal values (indicated by the hat sign). Some bounding lines of this three-dimensional ellipsoid are drawn using the residuals at the optimal solution and their sensitivities by the application of the linearisation method (Eq.11).

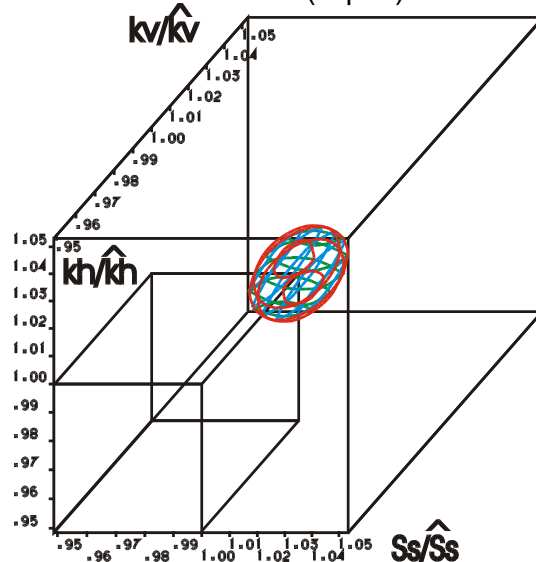


Figure 3 Three-dimensional ellipsoid which approximates the 99% joint confidence region of the hydraulic parameters

The largest principal axis of the ellipsoid is 4.3 times larger than the smallest principal axis of the ellipsoid whereas the second largest principal axis is 2.6 times larger than the smallest. This can also be deduced from the condition indexes  $\eta$  (Table 3). These principal axes are, however, not parallel with the parameter axes. The eigenvalues  $\beta$  of the variance-covariance matrix define the direction of the axes (Table 4). The first eigenvector corresponds with the projection of a unit length placed on the principal axis of the three-dimensional ellipsoid on the three parameter axes.

The problem is well-posed because the condition number (the largest condition index) is smaller than five. There is even no weak dependency among the columns of the sensitivities. The smallest condition index causes 98.81% of the marginal variance of the horizontal conductivity. The two largest

condition indexes cause almost exclusively the marginal variance of the two other hydraulic parameters. The sensitivities of the horizontal conductivities are almost completely independent from the sensitivities of the two other parameters. This can also be inferred from the correlation matrix. The smallest principal axis of the ellipsoid is almost parallel with the parameter axis of the horizontal conductivity as can also be deduced from the eigenvectors  $\beta$  (Fig. 3, Table 4). The somewhat larger dependency between the sensitivities of the other parameters can be deduced from the correlation matrix, the approximate joint confidence region, the eigenvalues of the covariance matrix and the matrix of marginal variance-decomposition proportions. This can also be derived from the three two-dimensional cross-sections through the ellipsoid (Fig.4).

Table 3 Condition indexes  $\eta$  and  $\Pi$  matrix of marginal variance-decomposition proportions due to the drawdown observations

$\eta$ Parameter	1.000	2.589	4.265
$k_h(1)$	0.9881	0.0114	0.0005
$k_v(1)$	0.0000	0.1122	0.8878
$s_s(1)$	0.0002	0.5090	0.4908

Table 4. Eigenvalues  $\alpha$  and eigenvectors  $\beta$  of the variance covariance matrix.

	$\alpha_1=.981 \times 10^5$	$\alpha_2=.361 \times 10^5$	$\alpha_3=0.539 \times 10^6$
$k_h(1)$	$\beta_{11}=0.6759$	$\beta_{12}=0.3639$	$\beta_{13}=-.9991$
$k_v(1)$	$\beta_{21}=-.6415$	$\beta_{22}=-.4760$	$\beta_{23}=-.0168$
$s_s(1)$	$\beta_{31}=0.3629$	$\beta_{32}=-.8006$	$\beta_{33}=-.0385$

### Addition of concentration sensitivities

After the optimisation of the parameter values with the drawdown observations the sensitivities of the concentration with respect to the three hydraulic

parameters (see part 1) are added to the sensitivity matrix of the drawdown (this part) after which the condition indexes and the matrix of marginal variance decomposition proportions are calculated (Table 5)

Table 5 Condition indexes  $\eta$  and  $\Pi$  matrix of marginal variance-decomposition proportions derived from drawdown and concentration sensitivities

$\eta$ Parameter	1.0000	2.379	3.551
$k_h(1)$	0.9812	0.0188	0.0000
$k_v(1)$	0.0001	0.6608	0.3391
$s_s(1)$	0.0001	0.7316	0.2683

By the addition of the information obtained through the concentrations observation the condition number of the problem becomes 3.551. This is smaller than in the problem where only the drawdown observations are considered. So, there is a gain in information by the addition of the concentration data. If it is assumed that the concentration residuals show similar distribution as the drawdown residuals then the marginal variance of the vertical conductivities becomes 1.47 times smaller; the marginal variance of the specific elastic storage becomes 1.27 times smaller; whereas the marginal variance of the horizontal conductivities stays practically unaltered. So, the marginal standard deviation of the vertical conductivities becomes 1.21 times smaller and those of the specific elastic storages 1.13 times.

The condition indexes and the matrix of the marginal variance decomposition proportions due to only the concentration sensitivities are given in Table 6. If one considers only the concentration data the hydraulic identification problem is less well posed. Its condition number is 13.7.

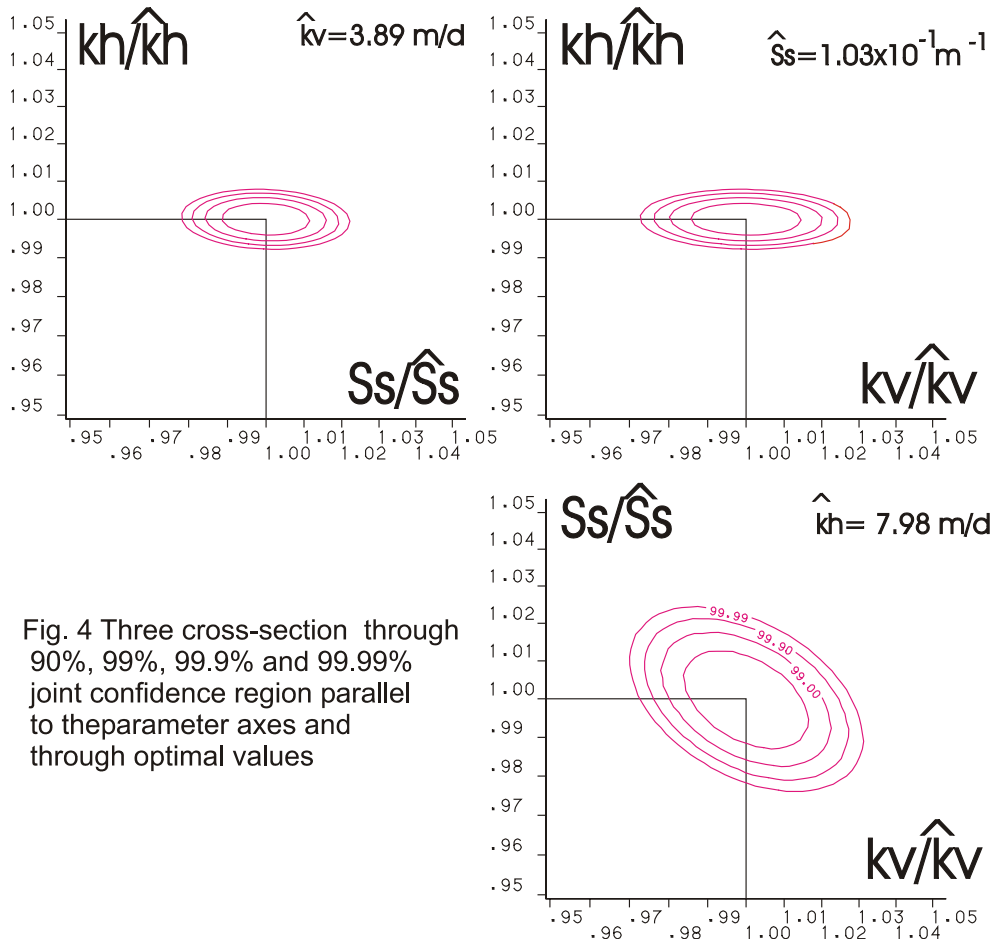


Fig. 4 Three cross-section through 90%, 99%, 99.9% and 99.99% joint confidence region parallel to the parameter axes and through optimal values

Table 6. Condition indexes  $\eta$  and  $\Pi$  matrix of marginal variance-decomposition proportions due to concentration observations alone

$\eta$	1.000	7.187	13.66
Parameter			
$k_h(1)$	0.0059	0.5287	0.4684
$k_v(1)$	0.0332	0.8619	0.1049
$s_s(1)$	0.0001	0.0405	0.9594

If the concentration residuals show the same distribution as the drawdown residuals and the hydraulic parameters are only inferred from the concentrations observations then the marginal variance of the horizontal conductivities becomes ten times larger than in the case that the drawdown observations are used. In this case the marginal variance of the vertical conductivities is 2.12 times larger than inferred from the drawdown observations whereas the marginal variance of the specific elastic storages will be 3.93 times larger. It is clear that the concentration data give

the most valuable data for the identification of the vertical conductivities. To a lesser extent information is provided for horizontal conductivity identification and in the smallest extent for the identification of the specific elastic storages.

Summarizing one can state that the vertical conductivity can be best identified from the concentration data whereas this parameter is the least identifiable from the drawdown data. The combination of both data sets results in a well-posed problem to identified the horizontal and vertical conductivities along with the specific elastic storages.

## CONCLUSIONS

The horizontal and vertical conductivities can be deduced from the drawdown observations along with the specific elastic storages. The used drawdowns are not only measured in

the directly pumped part of the aquifer but also in the layers above and below. With the inverse model based on an axial-symmetric numerical model the optimal values of the parameters can easily be reached after a limited number of iterations.

The approximate joint confidence region is a three-dimensional ellipsoid in the three-dimensional parameter space. The ratio of the principal axes with respect to the smallest axis correspond with the condition indexes. The drawdown observation results already in a well posed parameter identification problem. The horizontal conductivity can be inferred with the highest accuracy whereas the vertical conductivity with the smallest accuracy. By adding the concentration observation the problem is even better posed in which the vertical conductivities can be inferred with a higher accuracy than the specific elastic storages.

## REFERENCES

- Belsley, D.A. 1990. Conditioning diagnostics: collinearity and weak data in regression. New York: John Wiley & Sons.
- Boulton, N.S. 1963. Analysis of data from non-equilibrium pumping test allowing for delayed yield from storage. *Proc. Inst. Civ. Eng.* 26, 469-482
- Carrera, J. and S.P. Neuman, 1986. Estimation of aquifer parameters under transient and steady state conditions, 1, Maximum likelihood method incorporating prior information: *Water Resources Research* 22, no. 2, 199-210.
- Cooley, R.L. 1971. A finite difference method for unsteady flow on variably saturated process media, application to a single pumping well. *Water Resources Research* 7, no. 6, 1607-1625.
- Cooley, R.L. 1972. Numerical simulation of flow in an aquifer overlain by a water table aquitard. *Water Resources Research* 8, no. 4, 1046-1050.
- Cooley, R.L. and C.M. Case, 1973. Effect of a watertable aquitard on drawdown in an underlying pumping aquifer. *Water Resources Research* 8, no. 2, p. 434-447.
- Draper, N.R. and H.E. Smith. 1981. Applied regression analysis (2<sup>nd</sup> ed.). New York, John Wiley & Sons.
- Hantush, M.S., 1960. Modification of the theory of leaky aquifers. *Journ. Geophys. Res.* 65, 3713-3725.
- Hantush, M.S., 1966. Analysis of data from pumping tests in anisotropic aquifers. *Journ. Geophys. Res.* 71, 421-426.
- Hill, M.C. 1989. Analysis of the accuracy of approximate, simultaneous, nonlinear confidence intervals on hydraulic heads in analytical and numerical test case. *Water Resources Research* 25, no. 3, 520-535.
- Jacob, C.E., 1946. Radial flow in a leaky artesian aquifer. *Trans. Amer. Geophys. Union* 27, no. 2, 198-205.
- Lebbe, L. 1988. Execution of pumping tests and interpretation by means of an inverse model (in Dutch). Ghent, Geological Institute, Ghent University, thesis.
- Lebbe, L. 1999. *Hydraulic Parameter Identification: Generalized Interpretation method of single and multiple pumping tests*. Heidelberg, Springer-Verlag.
- Lebbe, L., and N. Van Meir. 2000. Hydraulic conductivities of low pervious sediments inferred from triple pumping test and observed vertical gradients. *Ground Water* 38, no. 1, 76-88.
- Lebbe, L., and W. De Breuck. 1995. Validation of an inverse model for the interpretation of pumping tests and a study of factors influencing accuracy of results. *Journal of Hydrology* 172, 61-84.
- Tarhouni, J. 1994. Modèle inverse tridimensionnel d'optimisation de paramètres hydrauliques des nappes aquifères: applications à l'échelle régionale et locale. Ghent, Ghent University, Ph.D.thesis.
- Theis, C.V., 1935. The relation between the lowering of the piezometric surface and the rate and the duration of discharge of a well using groundwater storage. *Trans. Amer. Geophys. Union*, 16, 519-524.